

Article

Pore-Filled Proton-Exchange Membranes with Fluorinated Moiety for Fuel Cell Application

Hyeon-Bee Song, Jong-Hyeok Park , Jin-Soo Park * and Moon-Sung Kang *

Department of Green Chemical Engineering, College of Engineering, Sangmyung University, Cheonan 31066, Korea; gusql1231@gmail.com (H.-B.S.); sbq6358@gmail.com (J.-H.P.)

* Correspondence: energy@smu.ac.kr (J.-S.P.); solar@smu.ac.kr (M.-S.K.); Tel.: +82-41-550-5383 (M.-S.K.)

Abstract: Proton-exchange membrane fuel cells (PEMFCs) are the heart of promising hydrogen-fueled electric vehicles, and should lower their price and further improve durability. Therefore, it is necessary to enhance the performances of the proton-exchange membrane (PEM), which is a key component of a PEMFC. In this study, novel pore-filled proton-exchange membranes (PFPEMs) were developed, in which a partially fluorinated ionomer with high cross-linking density is combined with a porous polytetrafluoroethylene (PTFE) substrate. By using a thin and tough porous PTFE substrate film, it was possible to easily fabricate a composite membrane possessing sufficient physical strength and low mass transfer resistance. Therefore, it was expected that the manufacturing method would be simple and suitable for a continuous process, thereby significantly reducing the membrane price. In addition, by using a tri-functional cross-linker, the cross-linking density was increased. The oxidation stability was greatly enhanced by introducing a fluorine moiety into the polymer backbone, and the compatibility with the perfluorinated ionomer binder was also improved. The prepared PFPEMs showed stable PEMFC performance (as maximum power density) equivalent to 72% of Nafion 212. It is noted that the conductivity of the PFPEMs corresponds to 58–63% of that of Nafion 212. Thus, it is expected that a higher fuel cell performance could be achieved when the membrane resistance is further lowered.

Keywords: proton-exchange membrane fuel cell; hydrogen-fueled electric vehicles; pore-filled proton-exchange membranes; partially fluorinated ionomer; porous polytetrafluoroethylene



Citation: Song, H.-B.; Park, J.-H.; Park, J.-S.; Kang, M.-S. Pore-Filled Proton-Exchange Membranes with Fluorinated Moiety for Fuel Cell Application. *Energies* **2021**, *14*, 4433. <https://doi.org/10.3390/en14154433>

Academic Editor: Ivan Tolj

Received: 30 June 2021

Accepted: 18 July 2021

Published: 22 July 2021

Publisher's Note: MDPI stays neutral with regard to jurisdictional claims in published maps and institutional affiliations.



Copyright: © 2021 by the authors. Licensee MDPI, Basel, Switzerland. This article is an open access article distributed under the terms and conditions of the Creative Commons Attribution (CC BY) license (<https://creativecommons.org/licenses/by/4.0/>).

1. Introduction

Proton-exchange membrane fuel cells (PEMFCs) have been considered as a competitive and promising power source for various vehicular and stationary applications due to their advantages, such as high energy generation efficiency, mild operation conditions, and dynamic load-following capability [1,2]. In particular, from the viewpoint of environmental conservation and sustainable energy utilization, much attention has been paid to electric vehicles using hydrogen as fuel worldwide. There is no doubt that PEMFC is the most important technology that determines the performance and commercialization of such hydrogen-fueled electric vehicles [3]. Meanwhile, proton-exchange membranes (PEMs) are one of the core components determining the performance and price of PEMFCs. The PEMs have been developed to possess high proton conductivity, low fuel diffusion, excellent chemical and thermal stabilities, good mechanical strength, and low manufacturing cost [4,5].

Currently, perfluorinated sulfonic acid (PFSA) ionomer membranes such as Nafion have excellent chemical/physical stabilities and high proton conductivity, so they are widely used as the electrolyte membranes for PEMFCs and redox flow batteries (RFBs) [6,7]. However, the high price and the performance degradation at elevated temperatures and low relative humidity are the obstacles to the commercialization of hydrogen-fueled electric vehicles. Therefore, non-fluorinated ionomer membranes with various structures have been

developed and excellent performances have been reported [1,4]. However, non-fluorinated ionomers still have relatively low chemical/physical stabilities compared to perfluorinated ionomers, and their performance needs to be further improved for commercialization. In this respect, partially-fluorinated ionomers could be manufactured at a lower price than perfluorinated ionomers which can still show dimensional stability and phase separation between hydrophobic and hydrophilic domains, and are also expected to improve chemical/thermal stabilities compared to non-fluorinated ionomers. For example, Mohammadi and Mehdipour-Ataei synthesized sulfonated partially fluorinated polysulfones which showed high conductivity, controlled dimensional swelling, and suitable thermal, mechanical, and oxidative stabilities [8]. In addition, the results of the membrane-electrode assembly (MEA) performance evaluation showed high current density and good stability in fuel cell conditions. Long et al. also synthesized sulfonated poly(arylene perfluoroalkylene) and prepared a PEM [9]. In particular, this was intended to confirm the effect of pendent multi-sulfonophenylene groups. The prepared PEM exhibited high ion-exchange capacity (IEC), great fuel cell performance under low-humidity conditions, and excellent durability. In addition, Jia et al. prepared a poly(arylene piperidinium) anion-exchange membrane (AEM) with a partially fluorinated backbone to control the swelling characteristics for application to alkaline fuel cells [10]. The prepared partially fluorinated AEM showed improved ionic conductivity, suppressed swelling, and excellent alkaline stability. However, it was also known that in the case of partially fluorinated polymers, depending on the structure, undesirable reactions such as dehydrofluorination may occur under harsh alkaline conditions [11].

Meanwhile, reducing the membrane thickness can be considered as an effective method for decreasing the ohmic loss caused by PEMs [12,13]. However, if the membrane thickness is reduced, it is difficult to obtain sufficient mechanical properties and low fuel crossover [4]. A pore filling method could overcome these problems [14–17]. The pore filling method is a membrane preparation technique filling monomer and crosslinker in the pores of a thin and tough porous substrate film, followed by thermal or UV curing. It allows the continuous preparation of a thin ion-exchange membrane having excellent dimensional stability and mechanical properties. It also has the advantage of significantly lowering the membrane's manufacturing cost. For example, Yamaguchi et al. prepared a pore-filled ion exchange membrane by filling poly(acrylamide-*tert*-butylsulfonic acid) into a cross-linked porous high-density polyethylene film for application to a direct methanol fuel cell (DMFC) [18]. The properties of the prepared pore-filled cation-exchange membrane (CEM) were greatly affected by the pore filling rate of the ionomer, and showed high proton conductivity and low methanol permeability compared to Nafion membranes. Wang et al. also developed a CEM by filling silane-crosslinked sulfonated poly(styrene-ethylene/butylene-styrene) into a porous polytetrafluoroethylene (PTFE) substrate for application to a direct alcohol fuel cell and direct formic acid fuel cell [19]. The prepared membranes exhibited a low liquid fuel crossover rate under the influence of the PTFE substrate, and confirmed excellent ionic conductivity and power density. In addition, Mong et al. synthesized sulfonated poly(arylene ether ketone) and filled it in a porous poly(arylene ether ketone) membrane to prepare a CEM [20]. As a result of analyzing the membrane properties for application to DMFCs, it showed superior thermal/dimensional stabilities and low methanol permeability compared to Nafion 117. Meanwhile, Kim et al. prepared a CEM by pore-filling poly(arylene ether sulfone)s on a crosslinked porous benzoxazine-benzimidazole copolymer substrate [21]. Due to the thin film thickness and the high content of chemically bound water molecules of the pore-filled membrane, it was confirmed that the PEMFC's properties under the above conditions were superior to those of the non-pore-filled membrane. Recently, Kim and Kang also reported a pore-filled AEM by filling a hydrophilic grade porous PTFE film with an anion-exchange polymer having high crosslinking density for the applications to an alkaline fuel cell using hydrazine fuel and a vanadium redox flow battery [22]. In particular, it was experimentally demonstrated that the hydrophilic/hydrophobic properties of the porous substrate used for the prepara-

tion of the pore-filled membrane have a significant effect on the MEA performance. The results clearly showed that the hydrophilicity of the pore-filled membranes was greatly influenced by the porous substrate, and the power generation performance of the alkaline fuel cell was significantly improved due to the reduction of the ohmic resistance of the membrane by increasing the hydrophilicity.

As a method to improve the performance of PEMs, in addition to partial fluorination, there are various effective membrane modification methods such as inorganic-organic hybrids and polymer blends, and they should compete with each other in terms of cost-effectiveness and performance improvement. From this sense, the pore-filling with partially fluorinated ionomer was considered as an economical and effective method to significantly improve the performance of PEMs. In this study, therefore, a porous PTFE substrate of hydrophilic grade was filled with a monomer including a proton-exchange group and a fluorinated monomer, and a pore-filled proton-exchange membrane (PFPEM) was fabricated through in-situ photo-induced polymerization. It was attempted to improve the chemical stability of the filling ionomer by copolymerizing a fluorinated monomer and increasing the cross-linking density by using a tri-functional cross-linking agent. In addition, by using a thin, tough, and hydrophilic porous substrate, it was expected to increase physical durability and at the same time lower the mass transfer resistance at the electrode-membrane interface. The prepared membrane was systematically analyzed through various physical, chemical, and electrochemical methods, and the PEMFC performance evaluation was also carried out using the MEAs employing the PFPEMs.

2. Materials and Methods

2.1. Materials and Membrane Preparation

2-Acrylamido-2-methylpropanesulfonic acid (AMSA) as a monomer containing a cation exchange group, 1H,1H,5H-octafluoropentyl methacrylate (OFPMA) as a fluorinated monomer, and diphenyl(2,4,6-trimethylbenzoyl)-phosphine oxide (TPO) as a photo-initiator were chosen and purchased from Tokyo chemical industry Co., Ltd. (Tokyo, Japan). In addition, trimethylolpropane triacrylate (TMPTA) as a tri-functional crosslinking agent and N,N-dimethylformamide (DMF) as a solvent were selected and purchased from Sigma-Aldrich Co. (St. Louis, MO, USA). All reagents used were used as received without further purification. We also chose Nafion 212 (DuPont, Wilmington, DE, USA) as the reference membrane to compare with the PFPEMs fabricated in this work.

Hydrophilic-grade porous PTFE film (thickness = ca. 30 μm , Advantec MFS, Inc., Tokyo, Japan) was used as the porous substrate for the membrane preparation. The specifications of porous PTFE substrate utilized for preparing PFPEMs are summarized in Table 1.

Table 1. Specifications of porous PTFE substrate utilized for preparing PFPEM in this work.

Substrate	Thickness (μm)	Pore Size (μm)	Porosity (%)
Hydrophilic PTFE (H020A142C)	ca. 30	0.2	71

For the preparation of the PFPEMs, monomer solutions, in which the mole ratios of OFPMA:AMSA were 1:0, 1:0.05, 1:0.1, 1:0.3, and 1:0.5, respectively, were prepared using a mixed solvent of DMF and distilled water (DW). The content of the cross-linker (TMPTA) was set at 10 wt% and TPO, used as an initiator for the photo-polymerization reaction, was added as 3 wt% to the total monomer solution. The porous PTFE substrate film was immersed in the monomer solution for a certain time so that the pores were completely filled with the monomers, followed by a photo-induced polymerization in a lab-made ultraviolet (UV) chamber (low pressure, lamp power = 40 W) for 20 min. The prepared membranes were converted into H^+ form by immersion in 1 M HCl for more than 24 h and stored.

2.2. Membrane Characterizations

The chemical synthesis of the partially fluorinated ionomer was confirmed by FT-IR (FT/IR-4700 equipped with an attenuated total reflectance accessory, Jasco, Tokyo, Japan) analysis. The morphological observation of the porous substrate and PFPEM was carried out with a field emission scanning electron microscopy (FE-SEM, JSM-7500F, JEOL Ltd., Tokyo, Japan). The hydrophilicity of the membrane surface was determined using a contact angle analyzer (Phoenix 150, SEO Co., Suwon, Korea). The water uptake of the membranes was determined using the following equation:

$$\text{Water uptake (\%)} = \left(\frac{W_{wet} - W_{dry}}{W_{dry}} \right) \times 100 \quad (1)$$

where W_{dry} and W_{wet} are the dry and wet weights of the membrane samples, respectively. For accurate measurement of dry membrane weight, the wet samples were dried in a vacuum oven at 40 °C for 24 h and weighed using a precision balance in a chamber in which humidity was kept constant (below 10% RH). An acid-base titration analysis was used to determine the IEC of the membrane samples. After the pre-equilibrium in a 0.5 M HCl, H^+ ions in the membrane sample were then fully exchanged with Na^+ ions in a 0.5 M NaCl. The amount of H^+ ions was then quantitatively determined by titration with a NaOH standard solution, and the IEC value was calculated using the following equation:

$$\text{IEC (meq./g}_{dry}m_{emb}) = \frac{N_{H^+} \cdot V_s}{W_{dry}} \quad (2)$$

where N_{H^+} is the normal concentration of H^+ (meq./L), V_s is the solution volume (L), and W_{dry} is the dry membrane weight (g). The proton conductivity (σ) was evaluated in a 0.5 M HCl solution at room temperature using a lab-made clip cell and an LCZ meter. Here, the membrane resistance was determined by subtracting the solution resistance from the measured resistance (i.e., membrane + solution). The proton conductivity of the membranes was also measured using a four-electrode in-plain conductivity cell (WonATech-ZIVE LAB, Seoul, Korea) connected to a potentiostat/galvanostat (SP-150, Bio-Logic Science Instruments, Seyssinet-Pariset, France). The impedance measurement was conducted at 70 °C under fully humidified conditions (100% RH). Nitrogen was supplied at 0.200 L min^{-1} at both sides of the channel during the measurement. The σ values were obtained from the following equation:

$$\sigma (\text{S/cm}) = \frac{l}{R_{memb} \cdot A} \quad (3)$$

where R_{memb} is the resistance (Ω), l is the thickness (cm), and A is the effective area (cm^2) of the tested membrane. The transport number (t_+) for counter ions (H^+) was obtained by measuring the cell potential with a lab-made two-compartment cell (membrane area = 0.785 cm^2 ; each volume = 0.23 dm^3) equipped with a pair of Ag/AgCl reference electrodes. As a result, the t_+ values were calculated by the following equation:

$$E_m = \frac{RT}{F} (2t_+ - 1) \ln \frac{a_L}{a_H} \quad (4)$$

where E_m is the cell potential, F the Faraday constant, T the absolute temperature, R the molar gas constant, and a_H and a_L the activity in high and low concentration compartments, respectively. The oxidative stability of the membranes was also evaluated by soaking the samples into Fenton's reagent (3% H_2O_2 containing 2 ppm $FeSO_4$) at 80 °C for 12 h. The time-course changes in the transport number and membrane weight were recorded to evaluate the alkaline and oxidative stabilities, respectively [23]. Thermal stability of the prepared membranes was checked by using a thermogravimetric analyzer (TGA-50, Shimadzu Co., Kyoto, Japan) in the temperature range of 25–600 °C under flowing nitrogen (50 $mL min^{-1}$). Tensile stress-strain curves of the membranes in the wet and dry states

were obtained by using a universal testing system (3340, Instron, Norwood, MA, USA). The I - V and chronopotentiometry curves were measured with a lab-made two-compartment cell equipped with a pair of Ag/AgCl reference electrodes and a pair of Ag/AgCl plate electrodes in a 0.025 M HCl solution [24].

2.3. PEMFC Performance Tests

Pt/C (TANAKA TEC10E50E, Pt 46.1%, TANAKA, Tokyo, Japan) was used as the electrocatalyst and Nafion D521 (Chemours, Wilmington, DE, USA) was used as the ionomer binder. For the catalyst ink, DW, 1-propanol, and 2-propanol (CARLO ERBA, Barcelona, Spain) were used as the solvents, and the solid content of the catalyst ink was fixed at 4.0 wt%. Catalyst layers for MEAs were coated on both sides of the membranes by using an auto spray machine (Nano NC, Seoul, Korea) and ultrasonic nozzles (Sono-Tek Corp., Milton, NY, USA). The active area was 9 cm², the electrocatalyst loading was 0.2 mg cm⁻², and the electrode ionomer/carbon ratio was fixed at 0.9. The unit cell evaluation was conducted using a unit cell and a fuel cell station (CNL Energy Corp., Seoul, Korea). A gas diffusion layer (250 μm, JNT20-A3, JNTG, Hwaseong, Korea) was utilized together with a graphite separator for the unit cell evaluation. The performance evaluation of the MEA was performed after 4 h of activation. During the performance evaluation, hydrogen and air were supplied at 0.254 and 0.805 L min⁻¹, respectively, and voltages were scanned at an interval of 0.05 V at 70 °C (100% RH) and 1 atm conditions. After the performance evaluation, impedance spectroscopy was performed through a potentiostat/galvanostat (SP-150, Bio-Logic Science Instruments, Seyssinet-Pariset, France), and hydrogen and air were supplied at 0.254 and 0.805 L min⁻¹, respectively, as in the performance evaluation. The analysis was performed under the conditions of 100.0 mHz–100.0 kHz (amplitude: 100 mV) at each voltage of 0.8, 0.7, 0.6, 0.5, and 0.4 V at 70 °C (100% RH) and 1 atm. Cyclic voltammetry (CV) was performed by using a potentiostat/galvanostat (SP-150, Bio-Logic Science Instruments, Seyssinet-Pariset, France) at 70 °C and 100% RH conditions and hydrogen and nitrogen were supplied at 0.200 L min⁻¹ during the measurement. The analysis was performed at a scan rate of 100.0 mV s⁻¹ at a voltage range of 0.1 to 1.2 V under 1 atm. Electrochemically active surface area (ECSA) through CV was calculated using the following equation:

$$\text{ECSA} \left(\text{m}^2 / \text{g}_{\text{Pt}} \right) = \frac{\text{Charge density} \left(\text{C cm}^{-2} \right)}{210 \left(\mu\text{C cm}_{\text{Pt}}^{-2} \right) \times \text{Pt content or loading} \left(\text{g}_{\text{Pt}} \text{ cm}^{-2} \right)} \quad (5)$$

Hydrogen gas crossover measurement was also conducted with a potentiostat/galvanostat (SP-150, Bio-Logic Science Instruments, Seyssinet-Pariset, France) at 70 °C (100% RH). Hydrogen and nitrogen were supplied at 0.200 L min⁻¹ during the measurement. The analysis was carried out at a scan rate of 1.0 mV s⁻¹ and a voltage range of 0.1 to 0.6 V under 1 atm.

3. Results and Discussion

Figure 1 shows the synthetic reaction scheme of the partially fluorinated proton-exchangeable polymer. As described in the experimental section, the molar ratio of OF-PMA/AMSA was controlled in the range of 0 to 0.5. In addition, since a tri-functional cross-linking agent (i.e., TMPTA) is used, high cross-linking density in the PEM can be expected.

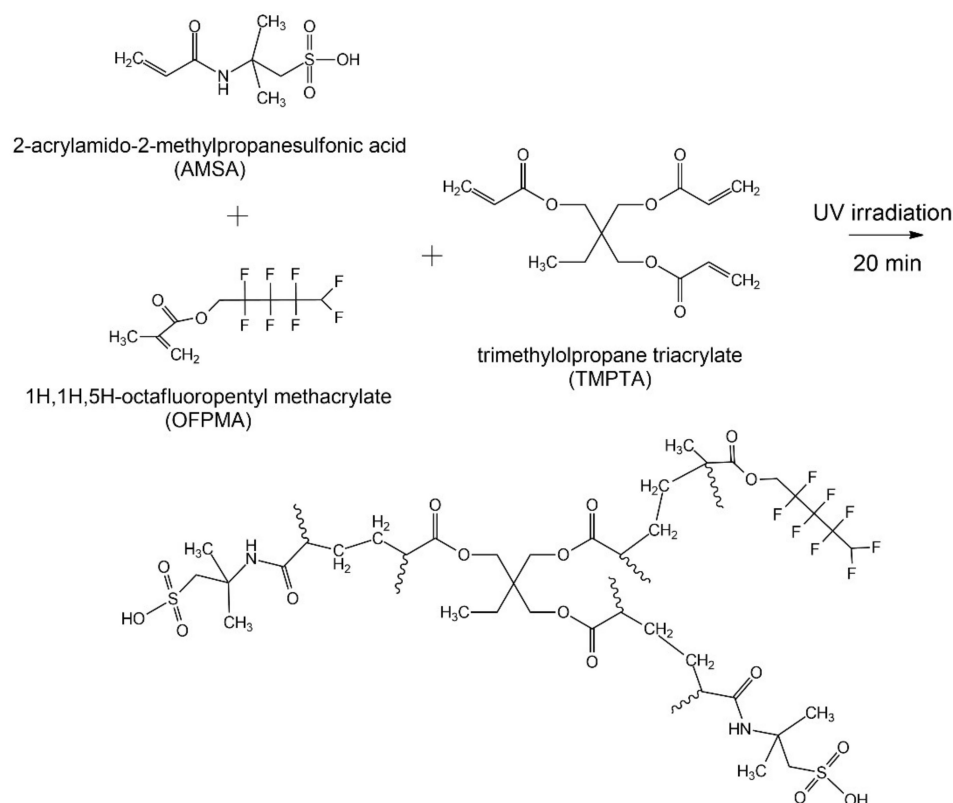


Figure 1. Reaction scheme of the cross-linked proton-exchangeable polymer containing fluorinated moiety.

The FE-SEM images of the porous substrate and prepared membrane are shown in Figure 2. A very well-developed pore structure can be observed from the surface and cross-sectional FE-SEM images (Figure 2a,c) of the porous substrate. However, in the images of the PFPEM (Figure 2b,d), it can be confirmed that the pores are completely filled with the ionomer formed by in-situ polymerization.

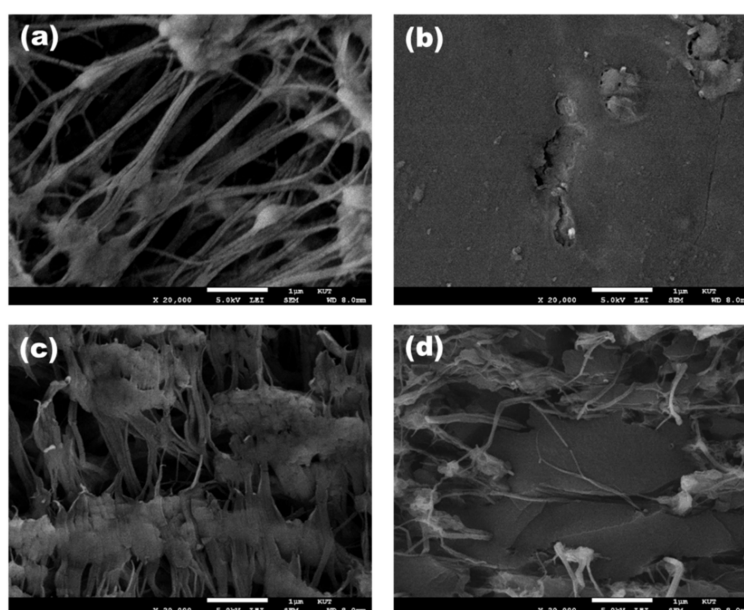


Figure 2. FE-SEM images of porous substrate and pore-filled membrane: surface—((a) PTFE porous substrate; (b) pore-filled membrane) and cross-section—((c) PTFE porous substrate; (d) pore-filled membrane).

Figure 3 shows the FT-IR spectra of the PTFE porous substrates and prepared pore-filled membranes. The two characteristic absorptions assigned to $-\text{CF}_2$ groups were found at 1203 and 1145 cm^{-1} in the spectra [25]. The absorption peak corresponding to the symmetric stretching ($\text{S}=\text{O}$) of sulfonate groups was also observed at 1045 cm^{-1} [26]. As the OFPMA/AMSA mole ratio is increased, it can be seen that the peak intensity of the $-\text{CF}_2$ groups increases and that of the $-\text{SO}_3^-$ groups decreases, simultaneously. Therefore, it can be confirmed that the partially fluorinated ionomer filled into the porous substrate was successfully synthesized according to the planned composition.

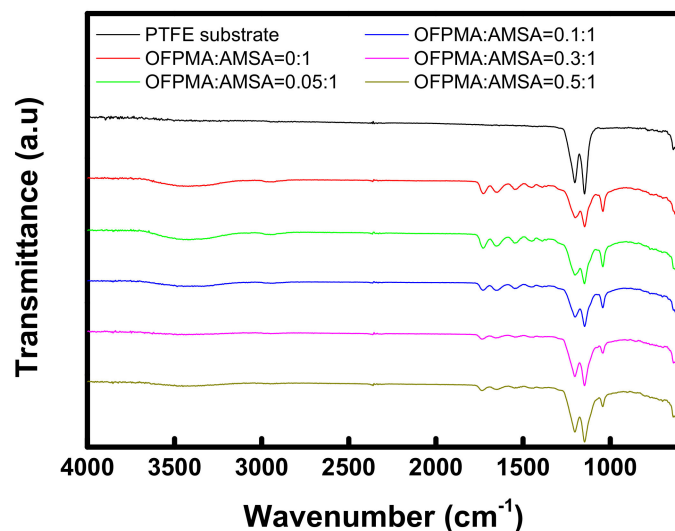


Figure 3. FT-IR spectra of the porous substrate and prepared membranes.

The basic performances of the commercial membrane (Nafion 212) and prepared PFPEMs are summarized in Table 2. In the case of water uptake, the PFPEMs showed higher values than Nafion in all conditions, and the values were also shown to decrease by increasing the OFPMA/AMSA mole ratio. Since the water uptake is strongly related to hydrophilic acid groups in the membrane, an increase in the OFPMA/AMSA mole ratio resulted in the reduction of the membrane water uptake by decreasing the hydrophilic phase. In the case of contact angle, except for the OFPMA:AMSA = 0:1 which does not contain a fluorinated monomer, it showed a relatively higher value than Nafion, but there was no significant difference. The surface hydrophilicity showed a tendency to decrease as the content of fluorinated monomer increased. The transport number indicating the ion selective permeability by the electrostatic force of the ion-exchange groups ($-\text{SO}_3^-$) was observed to be 0.96 or higher, which is the level of commercial membranes, for all membranes. As the content of fluorinated monomer increased, the transport number showed a tendency to somewhat decrease, indicating the weakened electrostatic force by decreasing the IEC. The proton conductivity measured at room temperature was shown to increase as the fluorinated monomer content decreased and the value of the OFPMA:AMSA = 0.5:1 was confirmed to be about 50% of that of Nafion 212. Similarly, the proton conductivity evaluated under a PEMFC operation condition ($70\text{ }^\circ\text{C}/100\%\text{ RH}$) was also revealed to be in the order of Nafion 212 (141.5 mS cm^{-1}) > OFPMA:AMSA = 0:1 (94.3 mS cm^{-1}) > OFPMA:AMSA = 0.5:1 (69.4 mS cm^{-1}). In fact, in this study, the experiment was performed by setting the IEC to a level similar to that of Nafion. It is believed that the lower proton conductivity compared to Nafion can be improved by increasing the IEC. It is also expected that the IEC of the PFPEMs can be increased by changing the structure and composition of the monomers and controlling the pore structure and porosity of the substrate.

Table 2. Various characteristics of commercial and prepared membranes.

Membranes	Nafion 212	OFPMA:AMSA = 0:1	OFPMA:AMSA = 0.05:1	OFPMA:AMSA = 0.1:1	OFPMA:AMSA = 0.3:1	OFPMA:AMSA = 0.5:1
Thickness (μm)	50.2 ± 0.43	26.4 ± 0.45	28.4 ± 0.25	27.9 ± 0.48	28.0 ± 0.72	27.2 ± 0.41
Water uptake (%)	18.1 ± 0.85	31.1 ± 0.83	29.0 ± 1.67	28.5 ± 2.19	25.0 ± 0.75	24.4 ± 0.82
Contact angle (degree)	50.1	45.3	51.6	54.7	55.6	56.5
IEC (meq/g)	1.08 ± 0.044	1.32 ± 0.04	1.30 ± 0.09	1.22 ± 0.03	1.18 ± 0.02	1.10 ± 0.05
Transport number (-)	0.985	0.981	0.980	0.977	0.977	0.968
Conductivity (S cm^{-1})	0.084	0.053	0.049	0.047	0.043	0.039

Figure 4 shows I - V curves and chronopotentiometry curves showing the electrochemical properties of the commercial membrane and PFPEMs. Both the I - V and chronopotentiometry curves exhibit typical polarization characteristics, so it can be concluded that all the tested membranes act as excellent ion selective barriers [24]. In addition, the difference among the samples in terms of the concentration polarization of membrane was shown to be within a normal experimental error range ($< \pm 5\%$) and no clear trend was found from the electrochemical responses displayed in Figure 4.

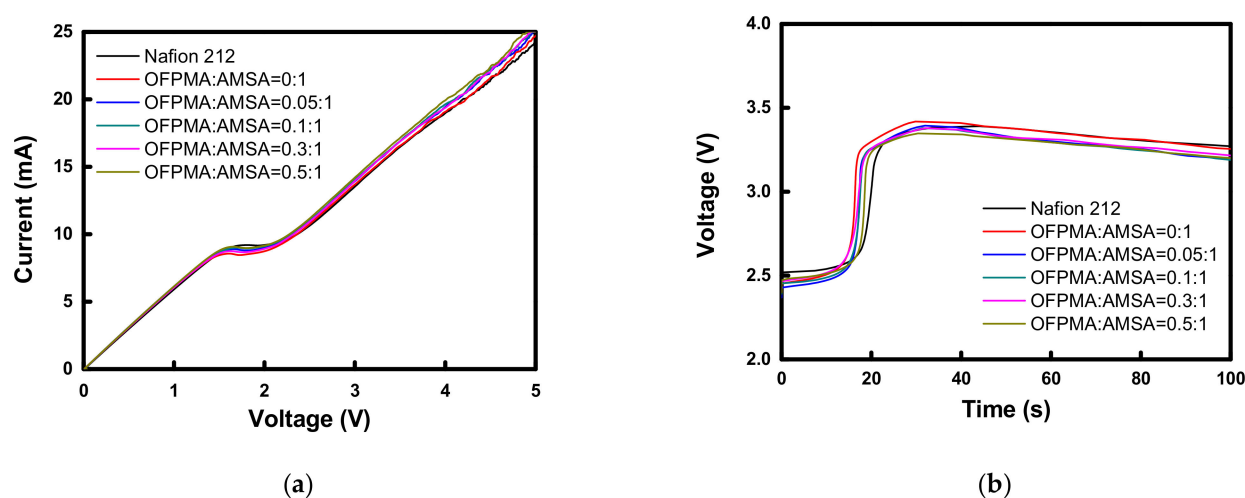
**Figure 4.** Electrochemical characteristics of commercial and prepared PFPEMs: (a) I - V curves; (b) Chronopotentiometry curves.

Figure 5 displays the tensile test results of the commercial membranes and prepared PFPEMs. It can be seen that despite the thinner thickness of the prepared PFPEMs compared to Nafion, they exhibit significantly greater toughness. In addition, it can be seen that the physical strength of the pore-filled membranes is not affected by the composition of the filling ionomer, because it is greatly influenced by the porous substrate used for the membrane fabrication.

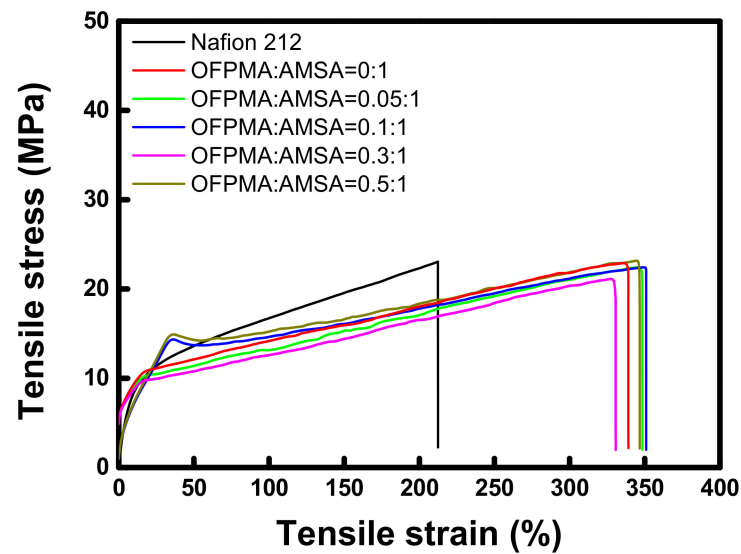


Figure 5. Tensile stress-strain curves of commercial membrane and prepared PFPEMs.

As revealed in Figure 6, the thermal stability of the commercial and prepared PFPEMs was evaluated as a function of the temperature, which was in the range of 25–600 °C. As a result, all the membranes were shown to be thermally stable up to 200 °C. Although there is a difference for each sample, the decrease in weight below 200 °C is considered to be due to the loss of $-\text{SO}_3\text{H}$ groups and water molecules adsorbed to the membrane [26]. However, no significant trend in weight loss was found among the membranes at 200 °C or lower. Above 200 °C, the PFPEMs started the decomposition of organic groups, which is faster than Nafion, but above 400 °C they showed superior thermal stability compared to that of Nafion. This is believed to be a result of the excellent thermal stability of the PTFE material used as the substrate.

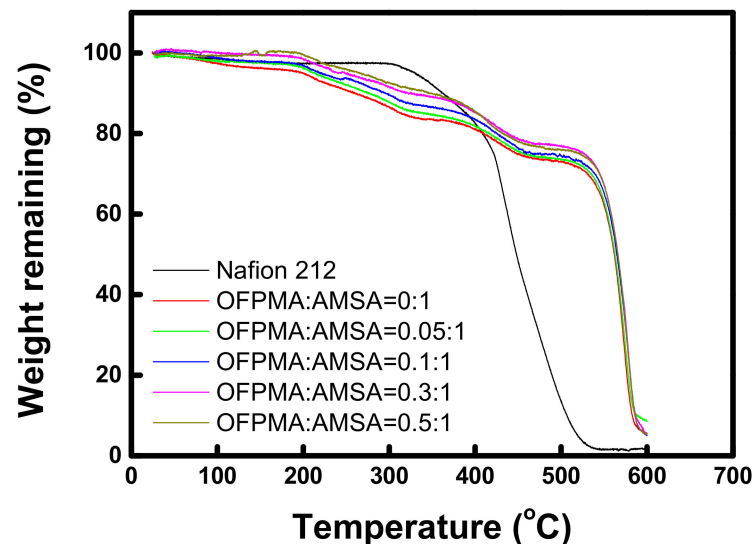


Figure 6. TGA curves of commercial membrane and prepared PFPEMs.

Time-course change in the residual weight of the commercial and prepared PFPEMs during the Fenton oxidation test (at 80 °C) is displayed in Figure 7. As a result, it was confirmed that the oxidation stability of the membrane was improved as the fluorine content was increased. That is, the OFPMA:AMSA = 0.5:1, which has the highest content of fluorinated monomer among the fabricated PFPEMs, showed the best oxidation stability, close to that of Nafion, a perfluorinated polymer. A fuel cell performance test was also

carried out with the composition OFPMA:AMSA = 0.5:1, which has rather low proton conductivity but the best oxidation stability.

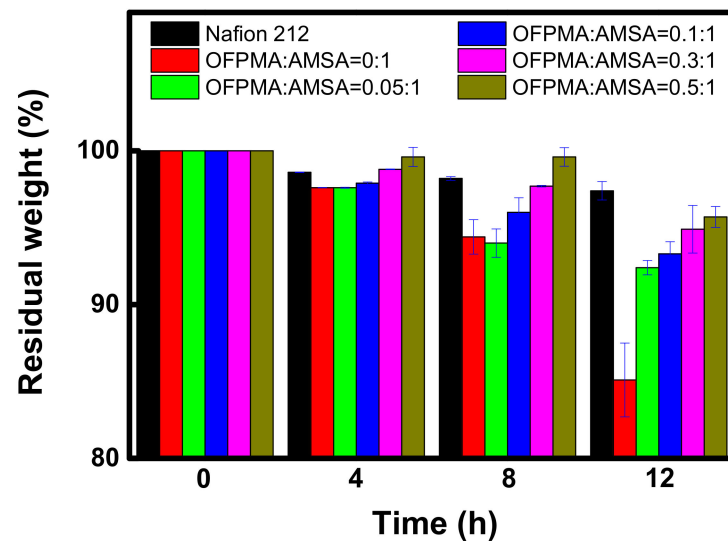


Figure 7. Time-course change in the residual weight of commercial and prepared PFPEMs during the Fenton oxidation test.

Figure 8 shows the results of the performance evaluation of the MEAs employing the Nafion 212 and PFPEMs, respectively. The fuel cell performance of the Nafion 212-based MEA shows the maximum power density, 466 mW cm^{-2} (at 847 mA cm^{-2}), and the PFPEM-based MEAs also exhibit excellent performances; 334 mW cm^{-2} (at 740 mA cm^{-2}) for OFPMA:ASMA = 0:1 and 340 mW cm^{-2} (at 679 mA cm^{-2}) for OFPMA:ASMA = 0.5:1. This result is interesting since the prepared PFPEM-based PEMFC performance (as maximum power density) shows 72% of Nafion 212 even though the conductivity of the PFPEMs corresponds to 58–63% of that of Nafion 212. However, the current density of the PFPEMs is still significantly lower than that of the Nafion membrane. This means that the proton conductivity of the PFPEMs needs to be further improved, and it is expected that this can be achieved by increasing the IEC and optimizing the pore structure and porosity of the substrate.

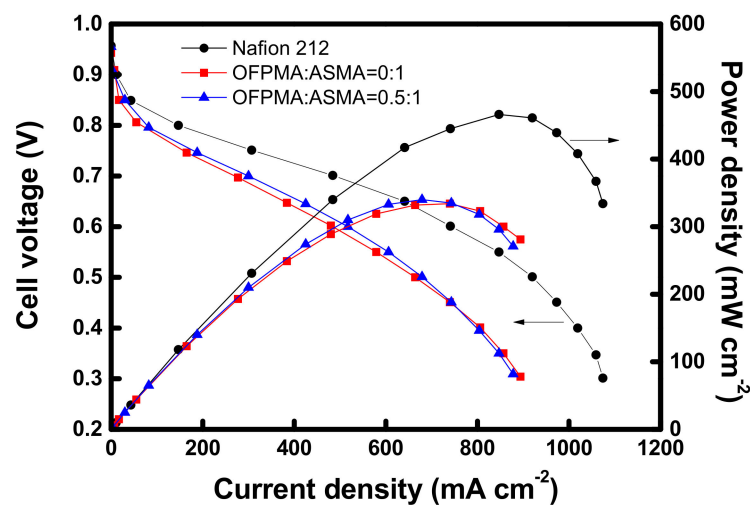


Figure 8. *I*-*V* and power density curves of the MEAs employing commercial membrane and prepared PFPEMs, respectively.

Figure 9 shows the results of the electrochemical impedance spectroscopy (EIS) analyses of the MEAs employing the commercial membrane and prepared PFPEMs, respectively.

Figure 9a reveals the HFR order of Nafion < OFPMA:ASMA = 0:1 < OFPMA:ASMA = 0.5:1. That is, the HFR has a correlation with the resistance of the electrolyte membrane, and the result was opposite to the order of the proton conductivity of the membranes. However, in the case of the CTR shown in Figure 9b, the OFPMA:ASMA = 0.5:1 exhibits the lowest resistance among the tested membranes at the reference potential of 0.6 V. That is, in case of the OFPMA:ASMA = 0.5:1, the membrane resistance was rather high, but by introducing a fluorine moiety into the membrane, the affinity with the perfluorinated ionomer utilized as an electrode binder could be increased. As a result, it is thought that the reduced membrane-electrode interfacial resistance resulted in the enhancement of the fuel cell performance.

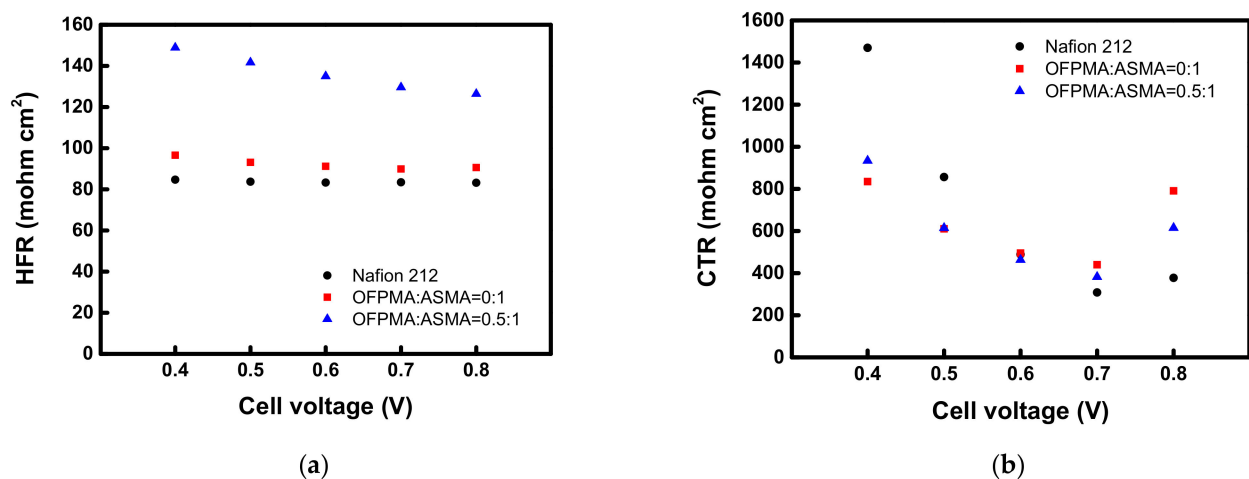


Figure 9. Electrochemical impedance spectroscopy analyses of the MEAs employing commercial membrane and prepared PFPEMs, respectively: (a) HFR vs. cell voltage; (b) CTR vs. cell voltage.

Figure 10a shows the cyclic voltammetry curve of the MEAs employing the commercial membrane and prepared PFPEMs. From these cyclic voltammetry curves, the electrochemically active surface area of the electrode can be estimated. The Nafion 212 shows the highest charge density (42.98 mC cm⁻²) and ECSA (102.3 m²_{pt}/g_{pt}), and the OFPMA:ASMA = 0:1 (32.30 mC cm⁻²; 76.90 m²_{pt}/g_{pt}), and OFPMA:ASMA = 0.5:1 (32.29 mC cm⁻²; 76.88 m²_{pt}/g_{pt}) revealed ca. 70% of the charge density and ECSA values, which corresponds to the result of the MEA performance. In addition, Figure 10b shows the measured hydrogen crossover current of the MEAs employing commercial membrane and prepared PFPEMs. As a result, the hydrogen crossover current density was maintained at less than 1.0 mA cm⁻² for all the tested membranes, and thus it can be confirmed that there are no pores or defects in the prepared PFPEMs.

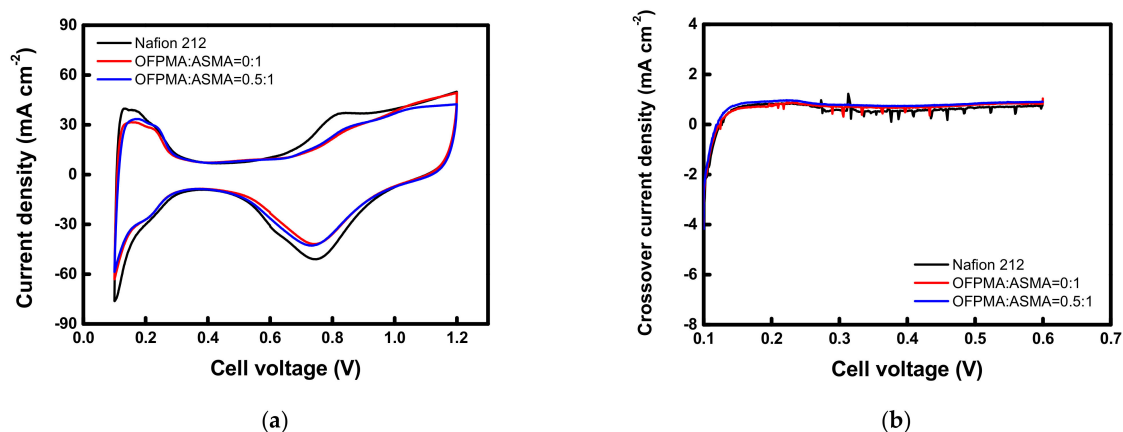


Figure 10. Electrochemical analyses of the MEAs employing a commercial membrane and prepared PFPEMs, respectively: (a) Cyclic voltammety curves; (b) Crossover current density vs. cell voltage.

4. Conclusions

In this study, low-cost and highly durable PFPEMs were successfully developed by combining a thin and tough porous PTFE substrate and a highly cross-linked partially fluorinated proton-exchange ionomer for PEMFC. AMSA was selected as a monomer containing proton-exchange groups, and OFPMA was chosen as a fluorinated monomer. In addition, tri-functional TMPTA was used as a cross-linking agent. A hydrophilic-grade PTFE porous film was employed as a porous substrate for the fabrication of the pore-filled membrane. The membrane fabrication was shown to be very simple and could be completed within 20 min. The prepared PFPEMs were systematically characterized through various methods and the performances were compared with those of Nafion 212, a commercially available perfluorinated sulfonic acid membrane. As a result, the proton conductivity was lower than that of Nafion 212. Nevertheless, the PFPEMs with 58–63% proton conductivity compared to Nafion 212 showed a PEMFC performance (as maximum power density) at 72% of that of Nafion 212. In particular, the PFPEMs exhibited excellent toughness despite the thin film thickness, and in the case of PFPEM with a fluorine moiety, the oxidation stability was greatly improved and good compatibility with a perfluorinated ionomer binder was also confirmed. As mentioned previously, the MEAs employing the PFPEMs exhibited somewhat lower current density and power density compared to those of Nafion. However, it is also expected that fuel cell performance at the level of Nafion will be possible when the PEM properties are optimized. In the future, research is planned to increase the fluorine content and the IEC, simultaneously, thereby lowering the membrane resistance.

Author Contributions: Conceptualization, M.-S.K. and J.-S.P.; methodology, M.-S.K. and J.-S.P.; experimentation, H.-B.S. and J.-H.P.; validation, M.-S.K.; investigation, M.-S.K. and J.-S.P.; resources, M.-S.K. and J.-S.P.; writing-original draft preparation, M.-S.K. and J.-S.P.; writing—review and editing, M.-S.K. and J.-S.P.; supervision, M.-S.K.; project administration, M.-S.K.; funding acquisition, M.-S.K. All authors have read and agreed to the published version of the manuscript.

Funding: This research was funded by a 2020 Research Grant from Sangmyung University (2020-A000-0228).

Institutional Review Board Statement: Not applicable.

Informed Consent Statement: Not applicable.

Data Availability Statement: Not applicable.

Acknowledgments: This research was supported by a 2020 Research Grant from Sangmyung University (2020-A000-0228).

Conflicts of Interest: The authors declare no conflict of interest.

References

1. Pan, M.; Pan, C.; Li, C.; Zhao, J. A review of membranes in proton exchange membrane fuel cells: Transport phenomena, performance and durability. *Renew. Sustain. Energy Rev.* **2021**, *141*, 110771. [[CrossRef](#)]
2. Giner-Sanz, J.J.; Ortega, E.M.; Pérez-Herranz, V. Hydrogen crossover and internal short-circuit currents experimental characterization and modelling in a proton exchange membrane fuel cell. *Int. J. Hydrog. Energy* **2014**, *39*, 13206–13216. [[CrossRef](#)]
3. Wang, G.; Yu, Y.; Liu, H.; Gong, C.; Wen, S.; Wang, X.; Tu, Z. Progress on design and development of polymer electrolyte membrane fuel cell systems for vehicle applications: A review. *Fuel Process. Technol.* **2018**, *179*, 203–228. [[CrossRef](#)]
4. Peighambari, S.J.; Rowshanzamir, S.; Amjadi, M. Review of the proton exchange membranes for fuel cell applications. *Int. J. Hydrog. Energy* **2010**, *35*, 9349–9384. [[CrossRef](#)]
5. Lim, S.; Park, J.-S. Composite membranes using hydrophilized porous substrates for hydrogen based energy conversion. *Energies* **2020**, *13*, 6101. [[CrossRef](#)]
6. Sánchez-Díez, E.; Ventosa, E.; Guarnieri, M.; Trovò, A.; Flox, C.; Marcilla, R.; Soavi, F.; Mazur, P.; Aranzabe, E.; Ferret, R. Redox flow batteries: Status and perspective towards sustainable stationary energy storage. *J. Power Sources* **2021**, *481*, 228804. [[CrossRef](#)]
7. Zhang, H.; Sun, C. Cost-effective iron-based aqueous redox flow batteries for large-scale energy storage application: A re-view. *J. Power Sources* **2021**, *493*, 229445. [[CrossRef](#)]
8. Mohammadi, M.; Mehdipour-Ataei, S. Durable sulfonated partially fluorinated polysulfones as membrane for PEM fuel cell. *Renew. Energy* **2020**, *158*, 421–430. [[CrossRef](#)]

9. Long, Z.; Miyake, J.; Miyatake, K. Partially fluorinated polyphenylene ionomers as proton exchange membranes for fuel cells: Effect of pendant multi-sulfophenylene groups. *ACS Appl. Energy Mater.* **2019**, *2*, 7527–7534. [[CrossRef](#)]
10. Jia, Y.; Ma, L.; Yu, Q.; Qaisrani, N.A.; Li, L.; Zhou, R.; He, G.; Zhang, F. Partially fluorinated, multication cross-linked poly(arylene piperidinium) membranes with improved conductivity and reduced swelling for fuel cell application. *Ionics* **2020**, *26*, 5617–5627. [[CrossRef](#)]
11. Ameduri, B. From vinylidene fluoride (VDF) to the applications of VDF-containing polymers and copolymers: Recent developments and future trends. *Chem. Rev.* **2009**, *109*, 6632–6686. [[CrossRef](#)] [[PubMed](#)]
12. Tsampas, M.N.; Pikos, A.; Brosda, S.; Katsaounis, A.; Vayenas, C.G. The effect of membrane thickness on the conductivity of Nafion. *Electrochim. Acta* **2006**, *51*, 2743–2755. [[CrossRef](#)]
13. Sun, C.-Y.; Zhang, H. Investigation of Nafion series membranes on the performance of iron—Chromium redox flow battery. *Int. J. Energy Res.* **2019**, *43*, 8739–8752. [[CrossRef](#)]
14. Kim, D.-H.; Kang, M.-S. Pore-filled ion-exchange membranes with optimal cross-linking degrees for efficient membrane capacitive deionization. *Macromol. Res.* **2020**, *28*, 1268–1275. [[CrossRef](#)]
15. Hwang, H.; Hong, S.; Kim, D.-H.; Kang, M.-S.; Park, J.-S.; Uhm, S.; Lee, J. Optimistic performance of carbon-free hydrazine fuel cells based on controlled electrode structure and water management. *J. Energy Chem.* **2020**, *51*, 175–181. [[CrossRef](#)]
16. Kim, D.-H.; Park, J.-S.; Choun, M.; Lee, J.; Kang, M.-S. Pore-filled anion-exchange membranes for electrochemical energy conversion applications. *Electrochim. Acta* **2016**, *222*, 212–220. [[CrossRef](#)]
17. Yun, S.-H.; Woo, J.-J.; Seo, S.-J.; Wu, L.; Wu, D.; Xu, T.; Moon, S.-H. Sulfonated poly(2,6-dimethyl-1,4-phenylene oxide) (SPPO) electrolyte membranes reinforced by electrospun nanofiber porous substrates for fuel cells. *J. Membr. Sci.* **2011**, *367*, 296. [[CrossRef](#)]
18. Yamaguchi, T.; Miyata, F.; Nakao, S. Polymer electrolyte membranes with a pore-filling structure for a direct methanol fuel cell. *Adv. Mater.* **2003**, *15*, 1198–1201. [[CrossRef](#)]
19. Wang, B.-Y.; Tseng, C.K.; Shih, C.-M.; Pai, Y.-L.; Kuo, H.-P.; Lue, S.J. Polytetrafluoroethylene (PTFE)/silane cross-linked sul-fonated poly(styrene-ethylene/butylene-styrene) (sSEBS) composite membrane for direct alcohol and formic acid fuel cells. *J. Membr. Sci.* **2014**, *464*, 43–54. [[CrossRef](#)]
20. Mong, A.L.; Yang, S.; Kim, D. Pore-filling polymer electrolyte membrane based on poly(arylene ether ketone) for enhanced dimensional stability and reduced methanol permeability. *J. Membr. Sci.* **2017**, *543*, 133–142. [[CrossRef](#)]
21. Kim, K.; Kim, S.-K.; Park, J.O.; Choi, S.-W.; Kim, K.-H.; Ko, T.; Pak, C.; Lee, J.-C. Highly reinforced pore-filling membranes based on sulfonated poly(arylene ether sulfone)s for high-temperature/low-humidity polymer electrolyte membrane fuel cells. *J. Membr. Sci.* **2017**, *537*, 11–21. [[CrossRef](#)]
22. Kim, D.-H.; Kang, M.-S. Pore-filled anion-exchange membranes with double cross-linking structure for fuel cells and redox flow batteries. *Energies* **2020**, *13*, 4761. [[CrossRef](#)]
23. Miyanishi, S.; Yamaguchi, T. Highly durable spirobifluorene-based aromatic anion conducting polymer for a solid ionomer of alkaline fuel cells and water electrolysis cells. *J. Mater. Chem. A* **2019**, *7*, 2219–2224. [[CrossRef](#)]
24. Kim, D.-H.; Choi, Y.-E.; Park, J.-S.; Kang, M.-S. Capacitive deionization employing pore-filled cation-exchange membranes for energy-efficient removal of multivalent cations. *Electrochim. Acta* **2019**, *295*, 164–172. [[CrossRef](#)]
25. Teng, X.; Dai, J.; Bi, F.; Yin, G. Ultra-thin polytetrafluoroethene/Nafion/silica composite membrane with high performance for vanadium redox flow battery. *J. Power Sources* **2014**, *272*, 113–120. [[CrossRef](#)]
26. Sun, C.; Zlotorowicz, A.; Nawn, G.; Negro, E.; Bertasi, F.; Pagot, G.; Vezzù, K.; Pace, G.; Guarnieri, M.; Di Noto, V. [Nafion/(WO₃)_x] hybrid membranes for vanadium redox flow batteries. *Solid State Ion.* **2018**, *319*, 110–116. [[CrossRef](#)]